

# 1 Approaching the low-frequency spectrum of rotating stars

Michel Rieutord

Laboratoire d'Astrophysique de Toulouse et Tarbes, UMR 5572, CNRS et  
Université Paul Sabatier Toulouse 3, 14 avenue E. Belin, 31400 Toulouse, France

**Abstract.** In this lecture I present the basic knowledge needed to understand the properties of the low-frequency spectrum of rotating stars. This spectrum is a mixture of inertial and gravity modes. These modes both have singularities in the limit of vanishing diffusion for a generic container. I explain the nature and the role of these singularities; I also discuss the way these modes can be computed and the actual difficulties that need to be circumvented to get sensible results.

## 1.1 Introduction

Rapidly rotating stars have benefitted from a renewed interest from stellar physicists as they have popped up in the observational fields of interferometry and asteroseismology.

Recent progress in interferometry allowed observers to measure the shape of a nearby star on the background sky, and for instance detect directly its centrifugal distortion. First successes were obtained by van Belle et al (2001) on Altair, but recent works give spectacular results on stars like Achernar (Domiciano de Souza et al, 2003), Altair (Domiciano de Souza et al, 2005; Peterson et al, 2006a; Monnier et al, 2007), and Vega (Aufdenberg et al, 2006). Observations not only give the angular diameters of the stars, but can also determine the orientation of the spin axis thanks to the measurement of the brightness distribution on the stellar surface.

These new observations are very important for stellar theory, because beyond the determination of the rotational distortion these data give access to the mass distribution inside a star, and all the physics which controls it.

Rotation long appeared as a key parameter in asteroseismology, as it permits the identification of modes by the famous rotational splitting. However, the recent launch of the CoRoT mission, the future launch of the KEPLER one, will strongly increase the precision of the measurements of stellar eigenfrequencies. The precision will be such that a parameter like rotation must perfectly be taken into account in the models, so that other quantities, like density, temperature... can be precisely constrained. It turns out that many stars thought to be not rapidly rotating, now fall in this category as the influence of rotation cannot be taken into account through a simple perturbative method. Sometimes, like for the slowly oscillating  $\gamma$ -Doradus stars, the rotation frequency is of the same order of magnitude as the excited eigenfrequencies. There too, rotation needs to be accounted for by direct, non-perturbative methods.

In the foregoing examples, two effects of rotation mix: the centrifugal distortion of the star and the Coriolis acceleration. The first one modifies the shape of the

star and mainly affects the high frequency acoustic oscillations, while the second one changes the low frequency part of the spectrum. In this series of lectures, the former is discussed by M.-J. Goupil, whereas we concentrate on the latter.

As a first step we shall discuss the case of plane waves propagating in a rotating fluid; we'll then naturally move on to the eigenmodes of rotating fluids, the so-called inertial modes, and also present the gravity modes, which share similar fundamental properties. This will bring us to the Poincaré equation, which controls these types of modes. The Poincaré equation being of hyperbolic type, we need to discuss in detail the various consequences of this property. We can then discuss the more complex case of gravito-inertial modes. We end this lecture by an introduction to the numerical methods which can be used to compute this part of the eigen spectrum of a rotating star.

## 1.2 Waves in a rotating fluid

### 1.2.1 Inertial waves

Inertial waves owe their existence to the Coriolis acceleration which serves as a restoring force and ensures the conservation of angular momentum. Let us consider the motion of a fluid particle under the action of this force. Its velocity verifies:

$$\frac{d\mathbf{v}}{dt} + 2\boldsymbol{\Omega} \wedge \mathbf{v} = \mathbf{0}$$

This equation is easily solved, and one finds

$$v_x = v_0 \cos(2\Omega t) \quad \text{and} \quad v_y = v_0 \sin(2\Omega t)$$

if at  $t = 0$ ,  $v_x = v_0$  and  $v_y = 0$ . The trajectory of the particle is also easily derived:

$$x = x_0 + \frac{v_0}{2\Omega} \sin(2\Omega t) \quad \text{and} \quad y = y_0 - \frac{v_0}{2\Omega} \cos(2\Omega t)$$

These expressions show that particles have a circular motion. The Coriolis acceleration thus brings the particles back to their equilibrium position after they have followed a circular trajectory of (Rossby) radius  $v_0/2\Omega$ .

### 1.2.2 Dispersion relation

Let us now consider waves propagating in an incompressible inviscid rotating fluid. The linearized equations of motion for disturbances read:

$$\frac{\partial \mathbf{v}}{\partial t} + 2\boldsymbol{\Omega} \wedge \mathbf{v} = -\frac{1}{\rho} \nabla P, \quad \nabla \cdot \mathbf{v} = 0$$

Choosing  $(2\Omega)^{-1}$  as the time scale and  $L$  as the length scale, we may rewrite these equations with dimensionless variables as

$$\frac{\partial \mathbf{u}}{\partial \tau} + \mathbf{e}_z \wedge \mathbf{u} = -\nabla p, \quad \nabla \cdot \mathbf{u} = 0 \quad (1.1)$$

Assuming that these waves are plane waves, i.e.

$$(p, \mathbf{u}) = (p, \mathbf{u})_0 e^{i(\omega\tau - \mathbf{k}\cdot\mathbf{x})},$$

incompressibility implies that:

$$\mathbf{k} \cdot \mathbf{u} = 0 \quad (1.2)$$

showing that the waves are transverse. The equation of momentum gives:

$$i\omega\mathbf{u} + \mathbf{e}_z \wedge \mathbf{u} = i\mathbf{k}P$$

from which we derive:

$$\begin{cases} \mathbf{e}_z \cdot (\mathbf{u} \wedge \mathbf{k}) = ik^2 P \\ i\omega u_z = ik_z P \\ i\omega \mathbf{k} \wedge \mathbf{u} = k_z \mathbf{u} \end{cases} \quad (1.3)$$

The dispersion relation of the waves follows from the elimination of the amplitudes:

$$\omega^2 = \frac{k_z^2}{k^2} \quad (1.4)$$

From this dispersion relation we first see that the pulsation of the waves is bounded up by the Coriolis frequency  $2\Omega$ , showing that the associated oscillations occupy the low-frequency part of the spectrum.

These waves propagate very anisotropically. Let us first derive the phase velocity; this is

$$\mathbf{v}_\phi = \frac{\omega}{k} \mathbf{e}_k = \frac{k_z}{k^3} \mathbf{k} \quad (1.5)$$

which shows that the phase prefers propagating along the rotation axis. Let us now compute the group velocity:

$$\mathbf{v}_g = \nabla_{\mathbf{k}} \omega(\mathbf{k}) = \frac{\mathbf{k} \wedge (\mathbf{e}_z \wedge \mathbf{k})}{k^3} \quad (1.6)$$

This relation shows that the group velocity is orthogonal to the phase velocity! Energy travels perpendicularly to the phase.

## 1.3 Inertial modes

### 1.3.1 General properties

The plane wave solution is acceptable only if the wavelength is very small compared to the size of the container. This is not necessarily the case, especially in astroseismology where one is interested in the global oscillations of stars. We thus need to consider the eigenmodes associated with these waves; still using the simplified set up of the incompressible inviscid fluid, the eigenfunctions verify

$$\begin{cases} i\omega\mathbf{u} + \mathbf{e}_z \wedge \mathbf{u} = -\nabla P \\ \nabla \cdot \mathbf{u} = 0 \\ \mathbf{u} \cdot \mathbf{n} = 0 \end{cases} \quad \text{on the boundary} \quad (1.7)$$

From this system we first derive the orthogonality property of these modes; if  $\omega_n$  and  $\omega_m$  are two different pulsations then

$$\int_{(V)} \mathbf{u}_n \cdot \mathbf{u}_m^* dV = 0 \quad (1.8)$$

because

$$\begin{cases} i\omega_n \mathbf{u}_n + \mathbf{e}_z \wedge \mathbf{u}_n = -\nabla P_n \\ -i\omega_m \mathbf{u}_m^* + \mathbf{e}_z \wedge \mathbf{u}_m^* = -\nabla P_m^* \end{cases} \quad (1.9)$$

which leads to

$$i(\omega_n - \omega_m) \int_{(V)} \mathbf{u}_n \cdot \mathbf{u}_m^* dV = 0$$

Moreover, as expected from the dispersion relation the spectrum is bounded:  $\omega \leq 1$ . This comes from

$$\omega = \frac{\int_{(V)} \text{Im}[(\mathbf{u}^* \wedge \mathbf{u}) \cdot \mathbf{e}_z] dV}{\int_{(V)} |\mathbf{u}|^2 dV}.$$

Using several times Schwarz inequality, it turns out that

$$|\omega| \leq \frac{\int_{(V)} |\text{Im}[(\mathbf{u}^* \wedge \mathbf{u}) \cdot \mathbf{e}_z]| dV}{\int_{(V)} |\mathbf{u}|^2 dV} \leq 1 \quad (1.10)$$

since  $|\text{Im}[(\mathbf{u}^* \wedge \mathbf{u}) \cdot \mathbf{e}_z]| \leq \|\mathbf{u}^* \wedge \mathbf{u}\| \leq \|\mathbf{u}\|^2$ . Thus again we find that inertial oscillations have a period larger than the semi-period of rotation.

Finally, let us note that when the spectrum exist<sup>1</sup> it is dense in the interval  $[0, 1]$ . A classical example of such a spectrum is:

$$\frac{n}{\sqrt{n^2 + m^2}}, \quad (n, m) \in \mathbb{N}^2$$

It is dense since any frequency in  $[0, 1]$  can be approximated to any precision by a pair of integers.

### 1.3.2 Rossby waves

When discussing waves in rotating fluids one often thinks to Rossby waves. What are they? Just a sort of inertial modes actually. As they play an important part in planetary atmospheres, they are often called planetary waves.

<sup>1</sup> Mentioned without precision, the spectrum means the point spectrum of an operator, that is, all the elements  $\lambda \in \mathbb{C}$  such that  $\mathcal{L}f = \lambda f$ , where  $f$  is square-integrable. For the Poincaré equation, the point spectrum is usually empty!

The idea is the following: we are looking for waves propagating in a very thin pellicula like the atmosphere of the Earth. We are seeking two-dimensional solutions (vertical motions are inhibited or much smaller than horizontal ones). The dispersion relation of such waves cannot be extracted from the one of the inertial waves since we impose to these new waves an additional constraint, namely  $v_z = 0$ . As any dispersion relation requires a simplification by an amplitude, this amplitude cannot be zero; we thus need to derive the dispersion relation from the beginning. Equations of motion are:

$$\begin{cases} i\omega \mathbf{v} + 2\Omega(y) \wedge \mathbf{v} = -\nabla P \\ \nabla \cdot \mathbf{v} = 0 \end{cases} \quad (1.11)$$

Note that now the rotation vector depends on  $y$  which is the North-South coordinate. Here we take a local frame where the  $x$ -axis points to the East and the  $z$  axis to the local zenith. Moreover, for two dimensional motions, the vertical component of the rotation vector is the only useful component. We thus write:

$$i\omega \mathbf{v} + 2\Omega(y) \mathbf{e}_z \wedge \mathbf{v} = -\nabla P$$

where  $\Omega(y) = \Omega \sin \lambda(y)$  and  $\lambda$  is the latitude; explicitly

$$\begin{cases} i\omega v_x - 2\Omega(y)v_y = -\frac{\partial P}{\partial x} \\ i\omega v_y + 2\Omega(y)v_x = -\frac{\partial P}{\partial y} \\ \frac{\partial v_x}{\partial x} + \frac{\partial v_y}{\partial y} = 0 \end{cases} \quad (1.12)$$

Pressure is eliminated for the vertical vorticity  $\zeta$ ; thus

$$i\omega \zeta = -2v_y \frac{d\Omega}{dy} \quad (1.13)$$

This equation shows that the latitude dependence of the rotation vector is crucial. We may now assume that  $\frac{d\Omega}{dy}$  is constant; this is the so-called  $\beta$ -plane approximation,  $\beta$  being the gradient of planetary vorticity. With this assumption, and setting  $(v_x, v_y) \propto \exp[i\omega t - ik_x x - ik_y y]$ , we easily get the dispersion relation of the Rossby waves:

$$\omega = -\frac{2k_x}{k_x^2 + k_y^2} \left( \frac{d\Omega}{dy} \right) \quad (1.14)$$

This relation shows that  $\omega/k_x < 0$  since  $\frac{d\Omega}{dy} > 0$ ; thus, Rossby waves are retrograde: they propagate in a counter-rotating way, to the West. The expression of their group velocity, namely

$$\mathbf{v}_g = 2 \frac{d\Omega}{dy} \left( (k_y^2 - k_x^2) \mathbf{e}_x + 2k_x k_y \mathbf{e}_y \right) / k^4$$

shows that energy propagates in all the directions.

The dispersion relation of these waves shows that the latitudinal variation of the rotation rate is crucial. Moreover, we may observe from the momentum equation

that even if the velocity field is that of a plane wave, this is not the case of the pressure perturbation since  $\frac{\partial P}{\partial x} \neq ik_x P$ .

As mentioned in introduction, it is clear that Rossby waves are just a specific type of inertial *mode* which meet some specific constraints like bidimensionality.

### 1.3.3 Planetary waves

Let us consider now a global analysis of the Rossby perturbations on the whole surface of the sphere. We would call these modes *planetary modes*. Since the flow is incompressible and two-dimensional, it can be described by a stream function  $\chi(\theta, \varphi)$ , such that

$$\mathbf{v} = \nabla \wedge (\chi \mathbf{e}_r)$$

$\mathbf{e}_r$  being the radial unit vector of spherical coordinates. We obtain the equation controlling  $\chi$  by applying the operator  $\mathbf{e}_r \cdot \nabla \wedge$  to (1.7). It turns out that

$$i\omega \mathbf{e}_r \cdot \nabla \wedge^2 (\chi \mathbf{e}_r) + \mathbf{e}_r \cdot \nabla \wedge (\mathbf{e}_z \wedge \mathbf{u}) = 0$$

which leads to

$$i\omega \Delta \chi + \frac{\partial \chi}{\partial \varphi} = 0$$

Now, if we expand the solutions onto spherical harmonics, namely

$$\chi = \sum_{\ell, m} \chi_m^\ell Y_\ell^m$$

we find that an eigenmode corresponds to each harmonic, with the eigen frequency  $\omega_{\ell m}$  following the dispersion relation

$$\omega_{\ell m} = \frac{m}{\ell(\ell+1)} \quad (1.15)$$

Note that we used the equation verified by spherical harmonics  $\Delta Y_\ell^m = -\ell(\ell+1)Y_\ell^m$ . We observe that the phase angular velocity is  $-\omega/m = -1/\ell(\ell+1)$  and always negative<sup>2</sup>. Thus, just like Rossby waves, planetary waves propagate to the West.

## 1.4 The Poincaré equation

Taking the divergence of the momentum equation in (1.7), we find the equation of the pressure perturbation, namely:

$$\Delta P - \frac{1}{\omega^2} \frac{\partial^2 P}{\partial z^2} = 0 \quad (1.16)$$

well-known under the name of *Poincaré equation* since Cartan (1922). Since  $\omega \leq 1$  this equation is spatially hyperbolic.

Before investigating the properties of this equation, let us make a stop on gravity modes, which also need the solutions of Poincaré equation.

<sup>2</sup> We indeed assumed that  $\chi$  is proportional to  $e^{i(\omega t + m\varphi)}$ .

### 1.4.1 A brief stop on gravity modes

Let us consider an incompressible stably stratified fluid (we use the Boussinesq approximation). Disturbances of the equilibrium verify the set of equations:

$$\begin{cases} \frac{\partial \delta \mathbf{v}}{\partial t} = -\frac{1}{\rho} \nabla \delta p + \frac{\delta \rho}{\rho} \mathbf{g} \\ \frac{\partial \delta T}{\partial t} + \delta \mathbf{v} \cdot \nabla T_0 = 0 \\ \nabla \cdot \delta \mathbf{v} = 0 \end{cases} \quad (1.17)$$

where  $T_0$  is the background temperature which we suppose to vary linearly with height  $z$ . We set

$$T_0 = T_{00} + \beta z \quad \text{with} \quad \beta > 0$$

For small variations of temperature

$$\frac{\delta \rho}{\rho} = -\alpha \delta T$$

where  $\alpha$  is the dilation coefficient of the fluid. The equations may be rewritten as

$$\begin{cases} i\omega \delta \mathbf{v} = -\nabla \delta p - \frac{N^2}{i\omega} \delta v_z \mathbf{e}_z \\ \nabla \cdot \delta \mathbf{v} = 0 \end{cases} \quad (1.18)$$

where we introduced the squared Brunt-Väisälä frequency, namely  $N^2 = \alpha \beta g$ . Assuming that  $N$  is constant and eliminating the velocity, we find:

$$\Delta_{x,y} \delta p - \left( \frac{\omega^2}{N^2 - \omega^2} \right) \frac{\partial^2 \delta p}{\partial z^2} = 0$$

which is the Poincaré equation, here again (note that for gravity modes  $\omega \leq N$ ).

### 1.4.2 Properties of the solutions of the Poincaré equation

The first important point is that Poincaré equation is hyperbolic with respect to space coordinates.

**A reminder about hyperbolic equations** Second order partial differential equations are divided into four categories: the elliptic, hyperbolic, parabolic and mixed types. This division is based on a property of the coefficients of the second order partial derivatives. Let us consider the general form:

$$A(x, y) \frac{\partial^2 f}{\partial x^2} + B(x, y) \frac{\partial^2 f}{\partial x \partial y} + C(x, y) \frac{\partial^2 f}{\partial y^2} + \dots = 0$$

The function  $D(x, y) = B^2 - 4AC$  determines the type of the equation. If everywhere in the definition domain of  $f$

- $D(x, y) > 0$ , the equation is hyperbolic
- $D(x, y) = 0$ , the equation is parabolic
- $D(x, y) < 0$ , the equation is elliptic

whereas if  $D(x, y)$  changes sign in the domain, the equation is said to be of *mixed type*. Examples:

- The wave equation is hyperbolic
- The heat equation is parabolic
- The equation of a potential is elliptic
- Tricomi's equation is of mixed type

**The consequences of hyperbolicity** The Poincaré problem is ill-posed in the sense of Hadamard: a hyperbolic problem is well-posed when associated with Cauchy type conditions, i.e. *initial conditions*. Boundary conditions are usually impossible to satisfy with  $C^\infty$  functions. We detail now some implications of ill-posedness.

① **Under-determination**

A first consequence of ill-posedness is that solutions are not fully determined. For instance, let us consider the wave equation

$$\frac{\partial^2 f}{\partial x^2} - \frac{1}{c^2} \frac{\partial^2 f}{\partial t^2} = 0$$

We all know that the general solution of this equation may be written

$$f(x, t) = \Phi(x - ct) + \Psi(x + ct)$$

where  $\Phi$  and  $\Psi$  are arbitrary functions. To be fully determined, they need two initial conditions, for instance,

$$f(x, 0) = \cos x \quad \text{and} \quad \left(\frac{\partial f}{\partial t}\right)_0 = 0$$

which leads to

$$f(x, t) = \frac{1}{2} [\cos(x - ct) + \cos(x + ct)]$$

Now, just imagine that instead of asking for two initial conditions to be met, we had been asking for one initial condition and a condition at some later time, just like:

$$f(x, 0) = I(x) \quad \text{and} \quad f(x, T) = F(x)$$

where  $I(x)$  and  $F(x)$  are given data. This problem is mathematically ill-posed and the solution cannot be fully specified. Indeed, we find that  $\Psi$  just has to satisfy

$$\Psi(x) = \Psi(x + 2cT) + F(x + 2cT) - I(x)$$

which means that this function needs to be given in the interval  $[0, 2cT]$ .

② **Infinite degenerescence**

An ill-posed problem may also have infinitely degenerate eigenvalues. For example, if one solves the (two-dimensional) Poincaré equation in a rectangle, namely

$$\frac{\partial^2 \psi}{\partial x^2} + \left(1 - \frac{1}{\omega^2}\right) \frac{\partial^2 \psi}{\partial z^2} = 0, \quad \psi = 0 \quad \text{on} \quad \partial \mathcal{D}$$

The classical solution is

$$\psi_{mn}(x, z) = A_{mn} \sin m\pi x \sin n\pi z$$

and

$$\omega_{mn}^2 = \frac{n^2}{m^2 + n^2} \tag{1.19}$$

The eigenvalues are infinitely degenerate because

$$\omega_{mn} = \omega_{jm, jn} \quad \forall j \in \mathbb{N}$$

and each eigenmode is arbitrary

$$\psi_{mn}(x, z) = \sum_{j=1}^{\infty} a_j \sin jm\pi x \sin jn\pi z$$

③ **Singularities**

If  $D(x, y) = B^2 - 4AC > 0$ , we can “factorize” the second order terms; hence,

$$A \frac{\partial^2 f}{\partial x^2} + B \frac{\partial^2 f}{\partial x \partial y} + C \frac{\partial^2 f}{\partial y^2} + \dots = 0$$

is changed into

$$\left(a \frac{\partial}{\partial x} + b \frac{\partial}{\partial y}\right) \left(a' \frac{\partial}{\partial x} + b' \frac{\partial}{\partial y}\right) + \dots = 0$$

which means that there exists a coordinate system  $(u, v)$  such that

$$\frac{\partial^2 f}{\partial u \partial v} + \dots = 0$$

with

$$\frac{\partial}{\partial u} = a \frac{\partial}{\partial x} + b \frac{\partial}{\partial y}$$

$$\frac{\partial}{\partial v} = a' \frac{\partial}{\partial x} + b' \frac{\partial}{\partial y}$$

$(u, v)$  are the *characteristic coordinates* and the curves  $u = \text{Cte}$  and  $v = \text{Cte}$  are the characteristic curves. They are two independent families of curves determined by the equations:

$$\frac{dy}{dx} = \frac{b}{a} \quad \text{and} \quad \frac{dy}{dx} = \frac{b'}{a'}$$

Let us now illustrate the foregoing discussion by an example where we impose boundary conditions to a wave-type equation. A typical situation is illustrated in Fig. 1.1. From this figure we see that



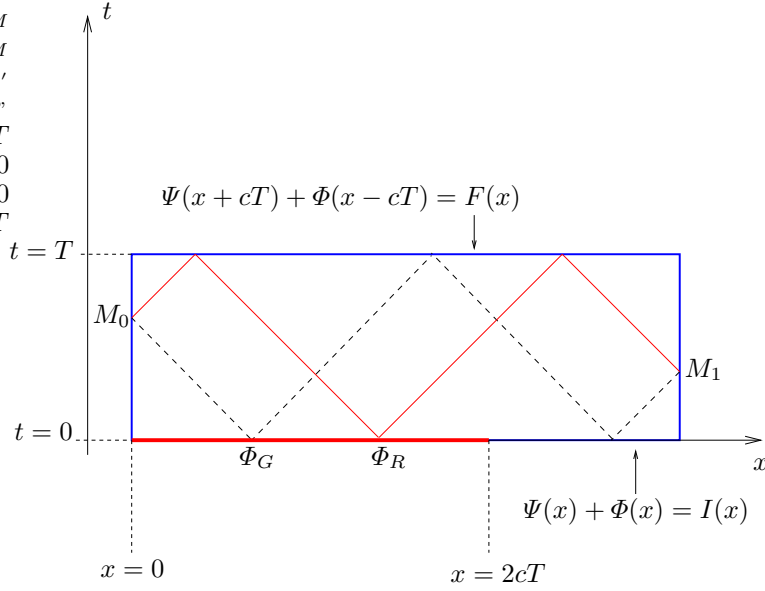


**Fig. 1.2.** Illustration of the compatibility of boundary conditions with a hyperbolic equation. If  $\Phi_G$  and  $\Phi_R$  are given, the values of the solution are known in  $M_0$  and  $M_1$ . But  $f(M_0)$  and  $f(M_1)$  are independent data which may not result from the same values of  $\Phi_G$  and  $\Phi_R$ .

**Attractors** Characteristics bounce on the boundaries of the domain and we may follow their trajectories just like those of a dynamical system in a phase space. However, this dynamics is very simple since the direction of the characteristics has only two possibilities:  $\pm\theta$ . In general, the trajectories converge towards an attractor as shown in Fig. 1.3. Attractors are specific to a container. The case of the spherical shell, more appropriate to astrophysical bodies, has been investigated in detail in Rieutord et al (2001). In the inertial frequency range  $[0, 2\Omega]$ , they may be characterized by the variations of their Lyapunov exponents.

### 1.4.3 The role of viscosity

The foregoing discussion ignored viscosity; however, as one can imagine, singularities are smoothed out by viscosity. Mathematically, when viscosity is restored, the problem is well-posed and solutions are said to be regularized. Nevertheless, one may wonder whether the singularities associated with attractors leave some signature in the viscous solutions. The answer is definitely yes, provided the viscosity is sufficiently small. As shown in Fig. 1.4, the eigenmode concentrates along the path of characteristics defined by the attractor: it generates an oscillating detached shear layer. The physical interpretation is that a wave packet launched randomly in the container, will rapidly be focused along the attractor. As time advances, it gets closer and closer to the attractor while its wavenumber increases until diffusion effects are strong enough to balance the contraction of the mapping made by the characteristics. This scenario has been used to derive analytical solutions of eigen

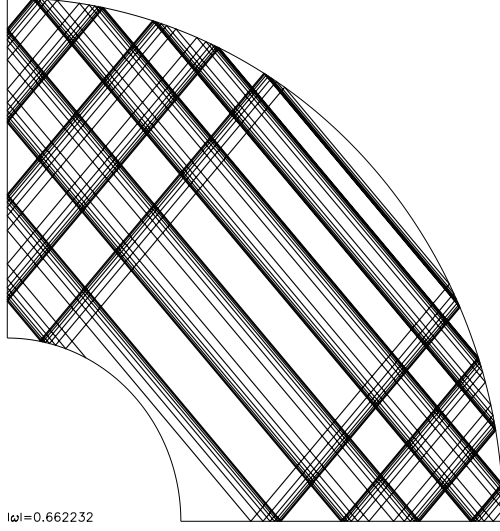


**Fig. 1.3.** Convergence of characteristics towards an attractor.

modes controlled by attractors (see Rieutord et al, 2002) in a two-dimensional case. In a thin shell, representing, for instance, the Earth atmosphere, attractors may be confined to equatorial regions and three-dimensional equations can be simplified into two-dimensional ones.

The structure of a detached shear layer (in the 2D case) can be derived from the system

$$\begin{cases} \lambda \mathbf{u} + \mathbf{e}_z \wedge \mathbf{u} = -\nabla P + E \Delta \mathbf{u} \\ \nabla \cdot \mathbf{u} = 0 \end{cases} \quad (1.21)$$

which controls the shape of inertial modes when there is viscosity (here given by the Ekman number  $E$ ). It turns out that the velocity in a shear layer is determined by the following differential equation:

$$\frac{d^2 u}{dz^2} - \left[ \frac{1}{4} z^2 + e^{i\pi/4} B \left( \frac{p}{2\alpha_0 A f_{20}} \right)^{1/2} (\tau_1 \pm i\omega_1) \right] u = 0$$

where  $z$  is the coordinate across the layer. This is actually the Schrödinger equation of a quantum particle trapped in a parabolic well, i.e. the famous harmonic oscillator. Its solutions are the parabolic cylinder functions:

$$u = U(a, z), \quad a = -n - \frac{1}{2} = e^{i\pi/4} B \left( \frac{p}{2\alpha_0 A f_{20}} \right)^{1/2} (\tau_1 \pm i\omega_1)$$

As shown in Rieutord et al (2002), the matching between these analytical solutions and the numerical ones is perfect. These solutions give for the first time (to our knowledge) an explicit example of the regularization of an operator.

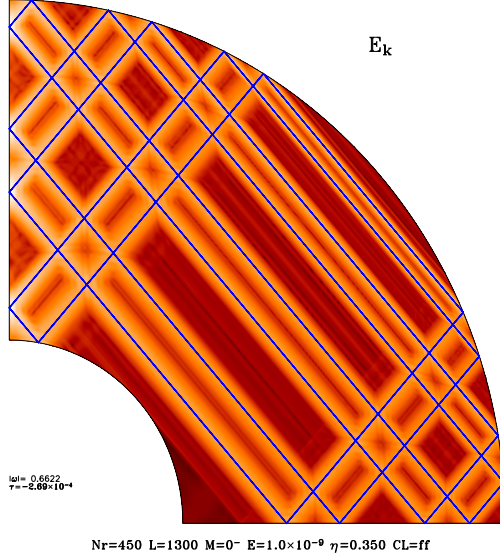


**Fig. 1.4.** An inertial mode focused around an attractor when the fluid is slightly viscous ( $E = 10^{-9}$ ).

#### 1.4.4 The critical singularity

The singularities issued from the characteristics attractors are very strong; solutions are neither integrable nor square-integrable. However, they are not the only singularities: some are associated with the boundary conditions. Indeed, for the inviscid case the velocity verifies  $\mathbf{v} \cdot \mathbf{n} = 0$  on the boundaries, which is equivalent to

$$-\omega^2 \mathbf{n} \cdot \nabla P + (\mathbf{n} \cdot \mathbf{e}_z)(\mathbf{e}_z \cdot \nabla P) + i\omega(\mathbf{e}_z \wedge \mathbf{n}) \cdot \nabla P = 0 \quad (1.22)$$

for the pressure. This condition is neither of Dirichlet type nor of Neumann type. It is called with “oblique derivatives”. It generates singularities at the so-called “critical latitude” which is where the characteristics are tangential to the boundary. This singularity is weaker than the attractor one (Rieutord et al, 2001) and usually manifests itself in a thickening of the Ekman boundary layer (e.g. Roberts and Stewartson, 1963).

#### 1.4.5 A remark on gravity modes

We have shown in sect. 1.4.1 that gravity modes are also governed by a hyperbolic equation. One may thus wonder why singularities of attractors have never been mentioned the astrophysical literature. The reason is that gravity modes have essentially been considered in non-rotating stars that are taken as perfect spheres. In such a geometry, the spherical symmetry of the problem makes the partial differential equations separable. Solutions are just the product of one-dimensional solutions

which are regular. Singularities disappear. We see that this situation is very specific and that singularities are rather the rule than the exception.

Finally, let us mention that singular gravity modes associated with attractors have been observed experimentally by Maas et al (1997), and are not a pure conjecture of theoretical work!

## 1.5 The gravito-inertial modes

In stars and other natural systems rotation and stable stratification usually act together. Since gravity modes and inertial modes are low-frequency modes, they always combine in the spectral range  $[0, \sqrt{(2\Omega)^2 + N_{\max}^2}]$ . In slowly rotating stars,  $N_{\max} \gg 2\Omega$  and there is a large number of gravity modes which are little affected by rotation; however, in rapidly rotating stars like  $\gamma$ -Dor, the Brunt-Väisälä frequency and the Coriolis frequency are of the same order of magnitude. The low-frequency modes need therefore a non-perturbative approach.

### 1.5.1 The mathematical side

The first question to be answered is how Poincaré equation is transformed when a stable stratification is combined with rotation. A simple way towards the answer is to consider a rotating radially stratified fluid in a sphere, and its small amplitude perturbations (e.g. Dintrans et al, 1999). Time-periodic disturbances are solutions of

$$\begin{cases} \nabla \cdot \mathbf{v} = 0 \\ i\omega \mathbf{v} + 2\boldsymbol{\Omega} \wedge \mathbf{v} = -\nabla p - \alpha T \mathbf{g} \\ i\omega T + \mathbf{v} \cdot \nabla T_0 = 0 \end{cases} \quad (1.23)$$

where  $\alpha$  is the dilation coefficient,  $T_0$  the background temperature which we take such that  $\nabla T_0 = \beta(r)\mathbf{e}_r$ . The local gravity is  $\mathbf{g} = -g(r)\mathbf{e}_r$ . When the temperature fluctuation is eliminated in favour of the velocity, the momentum equation reads:

$$i\omega \mathbf{v} + 2\boldsymbol{\Omega} \wedge \mathbf{v} = -\nabla p + \frac{N^2(r)}{\omega} i v_r \mathbf{e}_r \quad (1.24)$$

Taking the divergence of this equation, we get the generalization of the Poincaré equation. We write its second order terms for axisymmetric perturbations:

$$\begin{aligned} (\omega^2 - N^2(r) \cos^2 \theta) \frac{\partial^2 P}{\partial s^2} + 2N^2(r) \sin \theta \cos \theta \frac{\partial^2 P}{\partial s \partial z} \\ + (\omega^2 - N^2(r) \sin^2 \theta) \frac{\partial^2 P}{\partial z^2} + \dots = 0 \end{aligned}$$

where  $s$  is the radial cylindrical coordinate. These terms show the nature of the operator: it is of mixed type. The equation of the critical surfaces which separate the hyperbolic regions from the elliptic ones is

$$\omega^4 - (N^2(r) + 4\Omega^2)\omega^2 + 4\Omega^2 N^2(r) \cos^2 \theta = 0$$

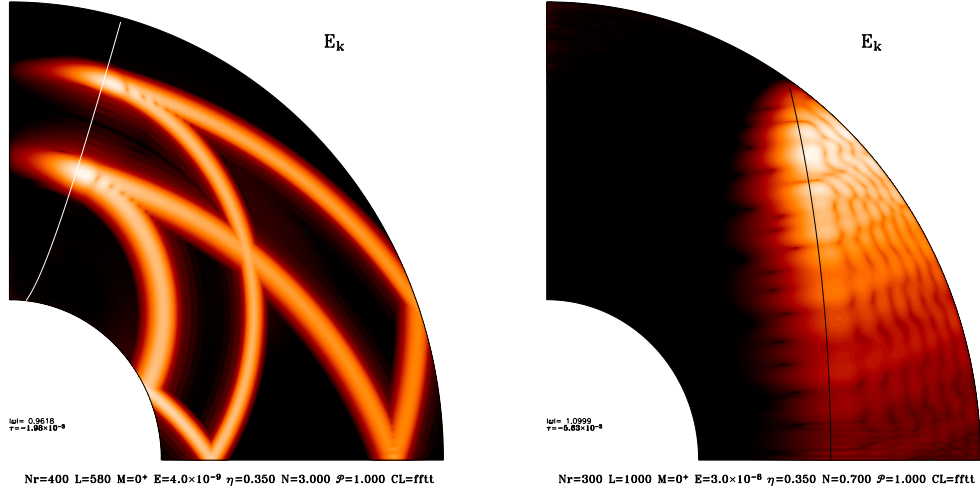


**Fig. 1.5.** Two examples of gravito-inertial modes confined in the hyperbolic region of the domain, shown by their kinetic energy amplitude in a meridional plane.

In some standard models (e.g. Rieutord, 2006; Chandrasekhar, 1961),  $N \propto r$ . In this case, critical surfaces are ellipsoid or hyperboloids.

In the hyperbolic regions, characteristics are no longer straight lines (in the meridional plane), but curves given by the following differential equation (e.g. Friedlander and Siegmann, 1982; Dintrans et al, 1999):

$$\frac{dz}{ds} = \frac{zsN^2 \pm \xi^{1/2}}{\omega^2 - N^2z^2}, \quad \xi = \omega^2 N^2 s^2 + (1 - \omega^2)(\omega^2 - N^2z^2) \quad (1.25)$$

Nevertheless, as before, the general rule is that they focus onto attractors. The novelty is that they are of two kinds: Either limit cycles of characteristics as before or a wedge made by a critical surface and a boundary. We give two examples of these modes in Fig. 1.5, for a Boussinesq model; others may be found in Dintrans et al (1999).

### 1.5.2 Gravito-inertial modes in stellar models

The foregoing discussion may be extended to more realistic models of stars. This exercise was done in Dintrans and Rieutord (2000) where we computed the gravito-inertial modes in a model of a  $1.8 M_{\odot}$ -ZAMS star. This mass is typical of the  $\gamma$ -Doradus stars.

By scanning the gravito-inertial frequency band, attractors have also been detected. They are limit-cycle attractors. However, we noticed some differences with the Boussinesq case. Namely, the frequency bands where attractors exist are noticeably narrower. The origin of this property is not clear yet, and may come from the “distance” between the Brunt-Väisälä frequency and the Coriolis frequency, i.e. for large-scale gravito-inertial modes, gravity dominates over rotation because  $N_{\max} \gg 2\Omega$ .

## 1.6 How can we compute these modes ?

To end this lecture, I would like to briefly address the numerical side of the subject. This is indeed a delicate question as the problem is two-dimensional and therefore involves large matrices.

The general form of the problem may be appreciated with the example of inertial modes. If we take the curl of the momentum equation in (1.21), we find that the velocity field verifies:

$$\lambda \nabla \wedge \mathbf{v} = E \Delta \nabla \wedge \mathbf{v} + \nabla \wedge (\mathbf{e}_z \wedge \mathbf{v}), \quad \nabla \cdot \mathbf{v} = 0$$

completed by boundary conditions. In a more symbolic form, this problem is a generalized eigenvalue problem, like

$$\mathcal{L}(f) = \lambda \mathcal{M}(f)$$

where  $\mathcal{L}$  and  $\mathcal{M}$  are partial differential operators and  $\lambda$  is the eigenvalue.

### 1.6.1 The grid

The first step in the numerical resolution is to decide about the discretization. In all the examples shown, we used spectral methods. These methods are indeed very appropriate since a discrete approximation of the functions is made in the most compact way. Thus, matrices have the smallest size for the required precision. This will appear as a key parameter.

Hence, for the horizontal part, we use a spherical harmonic expansion, while for the radial dependence, we use the Gauss-Lobatto grid, which is associated with Chebyshev polynomials. Typically, a function  $f(r, \theta, \varphi)$  is discretized in the following way:

$$f(r, \theta, \varphi) \equiv \sum_{\ell, m} f_m^\ell(r_i) Y_\ell^m(\theta, \varphi)$$

The set of  $f_m^\ell(r_i)$  constitutes the discrete representation.

### 1.6.2 The generalized eigenvalue problem

Once the discretization is fixed, the eigenvalue problem takes the form of the algebraic generalized eigenvalue problem  $[A]\mathbf{x} = \lambda[B]\mathbf{x}$ . This new problem can be solved numerically in three ways, typically. The first one is the brute force of the QR (real) or QZ (complex) algorithm where all the eigenvalues of the system are computed. Obviously, this can be done for small-size matrices only; the reasons are that the QR/QZ algorithm uses full matrices, thus the memory requirement is rapidly prohibitive as well as the computing time which grows like  $N^4$ ,  $N$  being the rank of the matrices.

When large sizes are necessary (for small diffusivities for instance), methods which determine a few eigenvalues of the spectrum are to be preferred. Indeed, the determination of the full spectrum does not make sense physically since we are

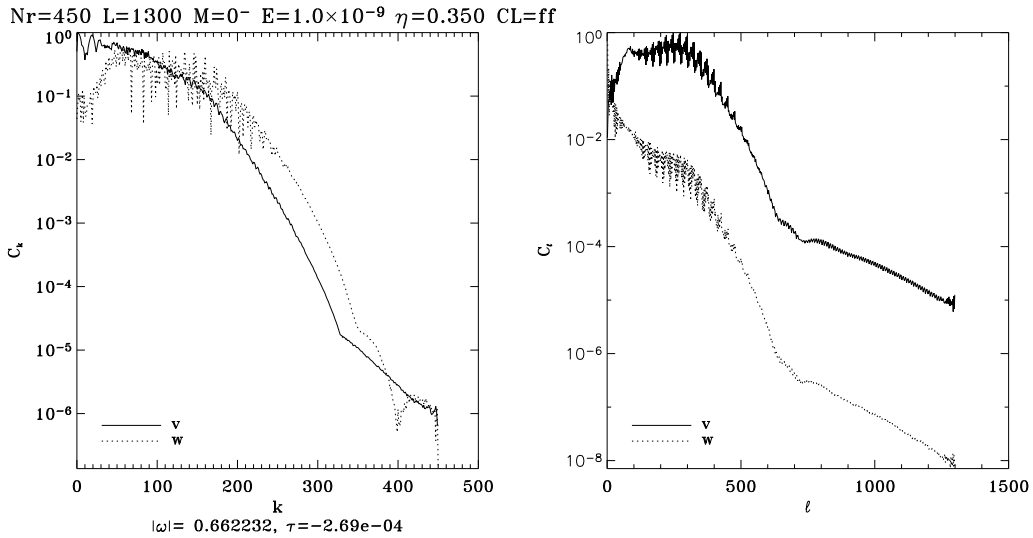


**Fig. 1.6.** Spectra of the numerical solution shown in Fig. 1.4. On left we see the amplitude of the Chebyshev coefficients (for the radial and azimuthal velocities). On right, we show the amplitudes of the spherical harmonics components for the same quantities.

usually interested in the least-damped modes; these modes are the ones which may be observed.

The method that we advise belongs to the Krylov-type methods, which iteratively determine the eigenvalues of some low-dimensional sub-space. We use the Arnoldi-Chebyshev algorithm (e.g. Valdettaro et al, 2007). In the same vein let us also mention the Jacobi-Davidson method which has been investigated more recently and may be more appropriate to parallel computers (e.g. Sleijpen and Van der Vorst, 2000).

### 1.6.3 Errors

However, once a solution is obtained, one needs to be sure that it is valid and not a spurious one. In other words, we must ascertain that the numerical error is negligible.

This error contains two independent sources of errors: the truncation error and the round-off error. The truncation error is the most obvious: spectral solutions are expansions in polynomials of higher and higher orders. Numerically, we use a finite number of such polynomials (equivalently, we use a finite number of grid points) and some difference remains with the exact solution. This *truncation* or *spectral* error is easily appreciated with a spectrum of the numerical solution as the ones shown in Fig 1.6. These two spectra represent the numerical solution of Fig. 1.4. We see the convergence of the solution on the Chebyshev polynomials and spherical harmonics basis. The truncation error is therefore  $\sim 10^{-5}$  (and less for other parts of the solution).

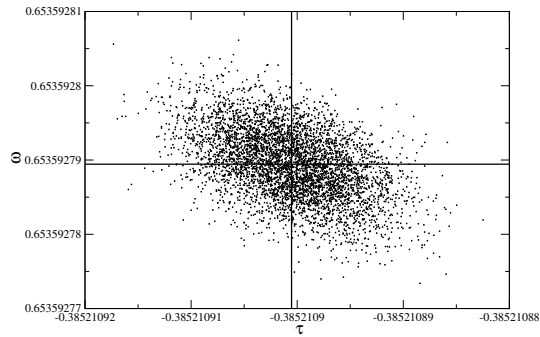


**Fig. 1.7.** Effects of the round-off error on the computation of an eigenvalue. The correct value, given by the cross, has been computed using extended precision computations (28-digits).

In the foregoing example, we may say that the numerical solution is spectrally converged. However, this solution may be pure junk if round-off errors dominate. Indeed, all calculations are done with a finite number of digits (typically 16 in double precision); unfortunately, it is quite common in numerical linear algebra, that the  $10^{-16}$  errors on the data are amplified by a factor  $10^{16}$  on the result. This comes from the conditioning of the matrices, which may be very bad. Such huge amplifications occur especially with ill-conditioned operators of large size. One way of estimating the round-off error on a numerical result consists in modifying the input data with a  $10^{-16}$ -noise. An example is given in Fig. 1.7 for the computation of an eigenvalue. A more detailed discussion, with examples, may be found in Valdetaro et al (2007).

## 1.7 Conclusions

To conclude this lecture, I would like to stress a few properties of the low-frequency spectrum of rotating stars, and some points in computing the associated eigenvalues and eigenmodes.

- In a general set-up, gravito-inertial modes, as understood by physicists, do not exist in an adiabatic approach. This is because the operator governing the eigenvalue problem is either spatially hyperbolic or of mixed type and is rarely compatible with boundary conditions.
- Diffusivities (viscosity or heat diffusion) therefore play an important part in the dynamics of the system. They regularize the singularities and control the size of the associated shear layers.
- When computing such modes, the singularity of the adiabatic limit shows up in the bad conditioning of the matrices of the associated linear systems. A careful control of the round-off error is therefore needed to obtain sensible results. Our experience is that the diffusion coefficients like viscosity are quite appropriate to improve the conditioning of the linear operators. Relying on numerical diffusion would be very hazardous.

Realistic numbers are often beyond reach of numerical solutions in astrophysical problems (just think to the Reynolds number in the convective zones of stars).

In the case of the eigenspectrum of a star, it turns out that the recent progress of computers' power together with that of numerical methods, makes the astrophysical regime within (indirect) reach of the calculations. Indeed, although the brute force computation is often not possible, the determination of the asymptotic laws governing a given eigenmode when diffusion numbers become small is possible in most cases. Thus, difficulties are to be expected from the models rather than from the eigenmode computation, although, as we have shown, this calculation is not an easy game.

I am very grateful to Coralie Neiner and Jean-Pierre Rozelot for the smooth organization of this school and the fruitful time spent there. The high resolution computations, illustrating this lecture, have been realized on the NEC-SX8 of the 'Institut du Développement et des Ressources en Informatique Scientifique' (IDRIS) which is gratefully acknowledged.



# Bibliography

- Aufdenberg JP, Mérand A, Coudé du Foresto V, Absil O, Di Folco E, Kervella P, Ridgway ST, Berger DH, Brummelaar TAt, McAlister HA, Sturmann J, Sturmann L, Turner NH (2006) First Results from the CHARA Array. VII. Long-Baseline Interferometric Measurements of Vega Consistent with a Pole-On, Rapidly Rotating Star. *ApJ* 645:664–675
- Cartan E (1922) Sur les petites oscillations d'une masse fluide. *Bull Sci Math* 46:317–352, 356–369
- Chandrasekhar S (1961) Hydrodynamic and hydromagnetic stability. Clarendon Press, Oxford
- Dintrans B, Rieutord M (2000) Oscillations of a rotating star: a non-perturbative theory. *A & A* 354:86–98
- Dintrans B, Rieutord M, Valdetaro L (1999) Gravito-inertial waves in a rotating stratified sphere or spherical shell. *J Fluid Mech* 398:271–297
- Domiciano de Souza A, Kervella P, Jankov S, Abe L, Vakili F, di Folco E, Paresce F (2003) The spinning-top Be star Achernar from VLTI-VINCI. *A & A* 407:L47–L50
- Domiciano de Souza A, Kervella P, Jankov S, Vakili F, Ohishi N, Nordgren TE, Abe L (2005) Gravitational-darkening of Altair from interferometry. *A & A* 442:567–578
- Friedlander S, Siegmann W (1982) Internal waves in a rotating stratified fluid in an arbitrary gravitational field. *Geophys Astrophys Fluid Dyn* 19:267–291
- Maas L, Benielli D, Sommeria J, Lam FP (1997) Observation of an internal wave attractor in a confined, stably stratified fluid. *Nature* 388:557–561
- Monnier JD, Zhao M, Pedretti E, Thureau N, Ireland M, Muirhead P, Berger JP, Millan-Gabet R, Van Belle G, ten Brummelaar T, McAlister H, Ridgway S, Turner N, Sturmann L, Sturmann J, Berger D (2007) Imaging the Surface of Altair. *Science* 317:342–, arXiv:0706.0867
- Peterson D, Hummel C, Pauls T, Armstrong J, Benson J, Gilbreath G, Hindsley R, Hutter D, Johnston K, Mozurkewich D, Schmitt H (2006a) Resolving the effects of rotation in Altair with long-baseline interferometry. *ApJ* 636:1087–1097
- Rieutord M (2006) The dynamics of the radiative envelope of rapidly rotating stars. i. a spherical boussinesq model. *A & A* 451:1025–1036
- Rieutord M, Georgeot B, Valdetaro L (2001) Inertial waves in a rotating spherical shell: attractors and asymptotic spectrum. *J Fluid Mech* 435:103–144
- Rieutord M, Valdetaro L, Georgeot B (2002) Analysis of singular inertial modes in a spherical shell: the slender toroidal shell model. *J Fluid Mech* 463:345–360
- Roberts P, Stewartson K (1963) On the stability of a maclaurin spheroid of small viscosity. *ApJ* 137:777–790

- Sleijpen G, Van der Vorst H (2000) A Jacobi-Davidson iteration method for linear eigenvalue problems. *SIAM Review* 42:267–293
- Valdettaro L, Rieutord M, Braconnier T, Fraysse V (2007) Convergence and round-off errors in a two-dimensional eigenvalue problem using spectral methods and arnoldi-chebyshev algorithm. *J Comput and Applied Math* 205:382–393, physics/0604219
- van Belle GT, Ciardi DR, Thompson RR, Akeson RL, Lada EA (2001) Altair's Oblateness and Rotation Velocity from Long-Baseline Interferometry. *ApJ* 559:1155–1164